

# First principles analysis on interaction between vacancy near surface and dimer structure of silicon crystal

Eiji Kamiyama<sup>a)</sup> and Koji Sueoka

Department of Communication Engineering, Okayama Prefectural University, 111 Kuboki, Soja, Okayama 719-1197, Japan

(Received 22 July 2011; accepted 17 December 2011; published online 12 January 2012)

We investigated the interactions between the dimer structures in a reconstructed Si (100) surface and a vacancy to understand the behavior of the point defects near the surface using first principles calculations. The calculated results showed that even a vacancy set in the ninth layer from the surface affects the charges around the dimers. This effect intensifies if the vacancy moves to the surface. Similar to the vacancies in a bulk, Jahn-Teller distortion occurred at atoms around the vacancy. When the introduced vacancy approaches to the fourth layer from the bottom, this distortion increased, and thus decreases the total energy. The third layer, in which forming a vacancy requires the highest energy, becomes a singularity layer in a Si (100) surface with dimer structures. The model, in which a vacancy was introduced into the fifth layer from the surface, came to have a vacancy in the fourth layer as an optimized structure due to a Si atom moving from the fourth to the fifth layer. We can see a clear interaction between the vacancy-originated charges and the surface dimer-originated one in this movement. As a consequence, the nature of the interaction between a surface dimer and a vacancy is intermediated by their accompanying charges. © 2012 American Institute of Physics. [doi:10.1063/1.3676265]

## I. INTRODUCTION

Bulk silicon (Si) wafers have been used as the base component of electronic devices for many years. Silicon-based composite substrates, such as Silicon-on-Insulator<sup>1–6</sup> and hybrid orientation technology<sup>7</sup> with direct-bonding wafers, have also started to be used as alternates for scaling devices. Nevertheless, a Si(100) surface plays an important role in today's devices when transistors are formed near the surface. Crystal surfaces are generally not only the sources but also the sinks of point defects, so it is important for us to understand their behaviors. The behavior of vacancies in a bulk Si crystal had been theoretically and experimentally investigated.<sup>8</sup> However, there are few reports about the vacancy behavior around the surface. Atoms near the Si surface have more freedom than the atoms inside that are far from the surface and they have shown unique behaviors.<sup>9</sup> Since a Si (100) surface tends to form dimers in order to decrease the number of dangling bonds and to become energetically stable,<sup>10</sup> point defects near the surface dimers must have unique behaviors, which is our final goal for understanding.

A Si (100) surface has two energetically equivalent asymmetric dimer structures and the flip-flop motions at room temperature between them are well-known.<sup>11</sup> This motion often causes the reconstructed Si (100) surface observed as a symmetric  $2 \times 1$  dimer structure when viewed from a scanning tunneling microscope (STM) at room temperature. As the sample cools to under 200 K, the flip-flop motions are frozen and the asymmetric dimer structures are revealed.<sup>12</sup> However, the ground state or the most stable structure at an ultra low temperature has not yet been identified. In this paper, there-

fore, we investigate the interactions between one vacancy and the  $c(4 \times 2)$  structure, one of the most stable dimer structures of a reconstructed Si (100) surface, as the first step to better understanding the behavior of point defects near the surface by first principles calculations.

## A. Simulation details

We fabricated a model of the  $c(4 \times 2)$  structures of a Si (100) surface, as shown in Fig. 1(a). In this model, the direction for infinitely arranging atoms in the bulk region is cut at the twelfth atomic layer from the surface, and the dangling bonds of atoms in that layer are terminated by hydrogen atoms. All the Si atoms in this model except for the ones at the surface were initially set in the optimized bulk position. Pairs of two Si atoms at the surface were set at the initial positions at a deviation of 0.5 Å from the bulk position along the opposite  $z$ - and  $x$ -directions. The bottom Si atoms and their terminating hydrogen atoms were constrained during the geometrical optimizations. After the geometrical optimizations of the model shown in Fig. 1(a), mono vacancy models were fabricated to remove one Si atom from each layer, accompanied by the numbers in Fig. 1(b). Then, geometrical optimizations were again performed for each mono vacancy model.

The calculations of the first principles analysis were based on the local density approximation<sup>13,14</sup> using the ultrasoft pseudopotential method<sup>15</sup> and the plane waves as a basis set for an efficient structure optimization. The expression proposed by Hammer *et al.*<sup>16</sup> was used for the exchange-correlation energy in the generalized gradient approximation (GGA). The CASTEP code was used to self-consistently solve the Kohn-Sham equation using the three-dimensional periodic boundary condition.<sup>17</sup> The density mixing method<sup>18</sup>

<sup>a)</sup>Electronic mail: ejkamiyama@aol.com.

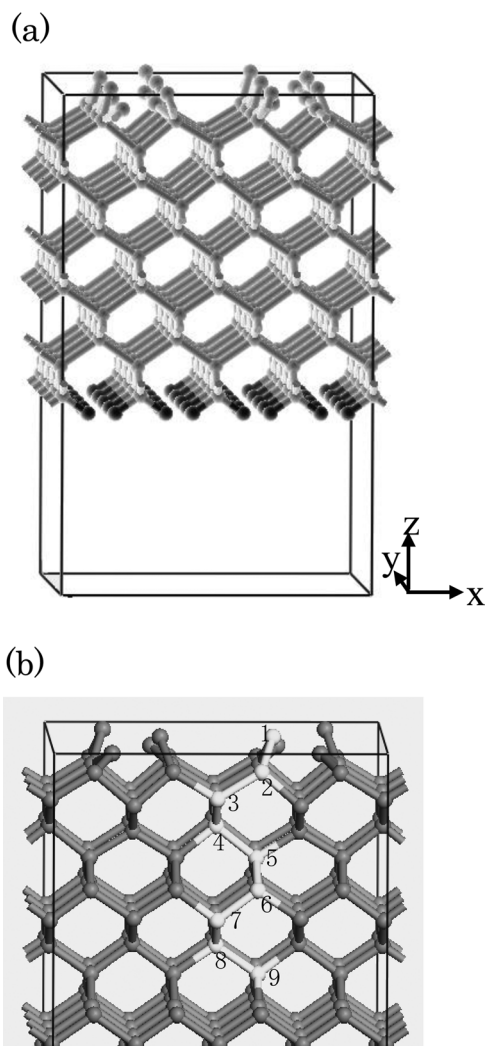


FIG. 1. (a) Model of  $c(4 \times 2)$  structures of Si (100) surface. The direction for infinitely arranging the atoms in the bulk region is cut in the twelfth atomic layer from the surface, and the dangling bonds of atoms in that layer are terminated by the hydrogen atoms. All the Si atoms in this model except for the surface Si atoms were initially set in the optimized bulk position. Pairs of two Si atoms on the surface were set at initial positions with a deviation of 0.5 Å from the bulk position along the opposite  $z$ - and  $x$ -directions. The bottom Si atoms and their terminating hydrogen atoms were constrained during the geometrical optimizations. (b) Mono vacancy positions fabricated by removing one Si atom from (a). The accompanied numbers show the actual position where a Si atom was removed and the layer number from the surface.

and BFGS geometry optimization method<sup>19</sup> were used to optimize the electronic structure and atomic configurations, respectively. Only the neutral charge state of the systems was considered in this study. The calculations were performed for the system at a temperature of absolute zero. Additionally, the  $k$ -point sampling was  $2 \times 2 \times 1$  special points of the Monkhorst-Pack grid.<sup>20</sup> The cutoff energy of the plane waves was 310 eV. The electric charges of the atoms for the optimized structures of each model were calculated using the Mulliken method.<sup>21</sup>

## B. Results and discussion

Figure 2 shows the increased total energies when introducing a vacancy in each layer. These energies come from changes in the number of Si atoms from the “before-

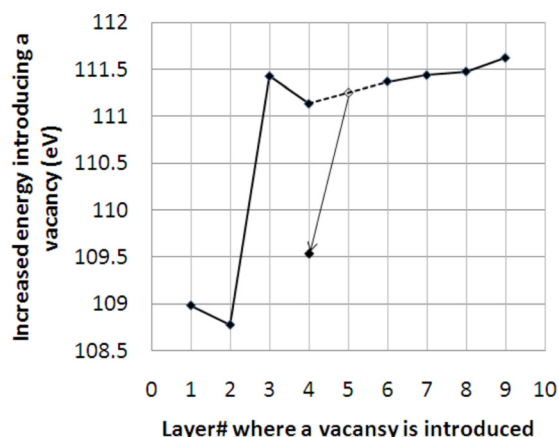


FIG. 2. (Color online) Energies increased by introducing of vacancy in each layer. The model, in which a vacancy is introduced in the fifth layer from the surface, created a vacancy in the fourth layer as an optimized structure by moving a Si atom from the fourth to the fifth layer. Total energy of the obtained structure is also much lower than that of the original” vacancy in the fourth layer” model shown in Fig. 1(b).

introducing V”-model to the “after-introducing V”-model. The corresponding energy in a bulk model is about 111 eV, which is near the values of 3rd–8th layers in Fig. 2. Using this value, we estimated the formation energy of a vacancy in a Si bulk crystal at about 3.5 eV, which is close to the experimentally obtained formation energy of a vacancy in Si bulk crystal. In a surface model such as Fig. 1, unfortunately, it is impossible to calculate the formation energy of a vacancy because not all Si atoms are equivalent.

In this figure, the model, in which a vacancy is introduced in the fifth layer from the surface as an initial structure, came to have a vacancy at the fourth layer as an optimized structure due to a Si atom moving from the fourth to the fifth layer. The vacancy of this obtained model is in a different arrangement with dimer atoms from that of the original model shown as the fourth layer in Fig. 1(b). The total energy of the obtained structure is also much lower than that of the original model. The total energies constantly increase from “a vacancy in the fourth layer” if a vacancy is introduced in the lower layer except for in the fifth layer model. In contract, the total energies of “a vacancy in the first and second layers” models are the lowest among all the calculated models. These phenomena will be discussed later.

Figure 3 shows an example of a comparison of the charges for each atom between the models: (a) without a vacancy and (b) with a vacancy introduced in the eighth layer. The surface dimers caused changes in the charges from the neutral states in the atoms down until the fourth layer. The vacancy in Fig. 3(b) also shows the changing area of the charge from the neutral state around one atomic layer. The charges seemingly originating from the vacancy in the eighth layer are separate from those of the surface dimers. However, this does not mean that no interaction exists between the vacancy and the dimers. Furthermore, if a vacancy exists closer to the dimers, the charges originating from them will be mixed.

The changes in the charges of the atoms from the first to the fourth layers against the vacancy position are shown in Fig. 4: A vacancy is introduced in the (a) first layer, (b)

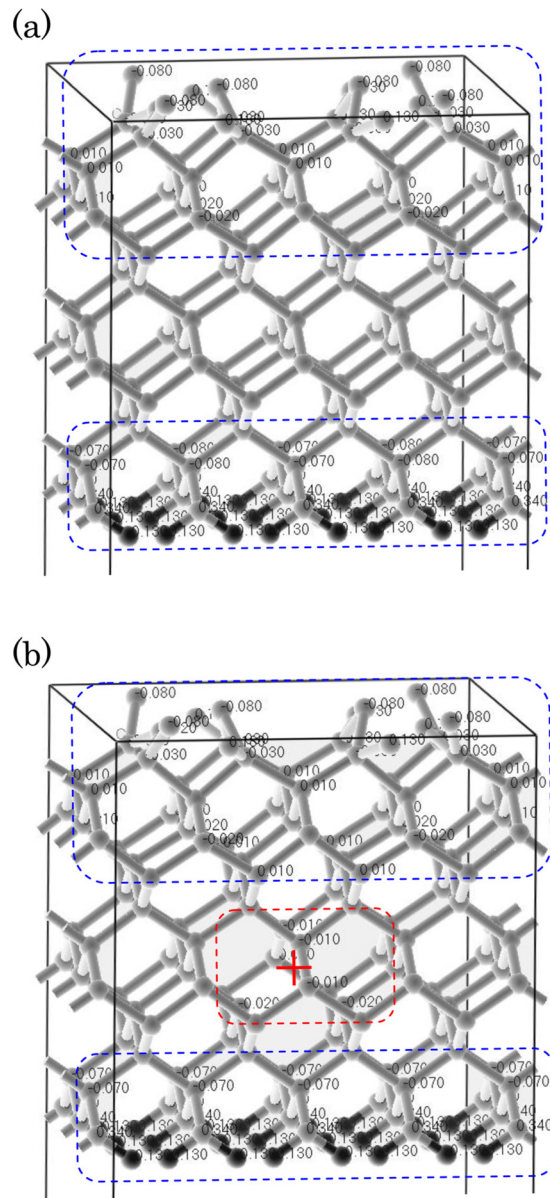


FIG. 3. (Color online) Example of comparison of charges for each atom between models: (a) without vacancy and (b) with vacancy introduced in eighth layer. The original vacancy position is marked with a crossing line. Charges surrounded by dot line in the top part originate from dimers. Charges surrounded by dot line in the bottom part originate from termination by hydrogen atoms. Charges surrounded by dot line in the center part of (b) originate from a vacancy.

second layer,..., (h) ninth layer, and (i) nowhere. These figures are top views, as viewed from the surface, and the projections of the original vacancy positions are marked with crossed lines. In Figs. 4(a)–4(h), the different numbers of charges from the “no vacancy model,” i.e., Fig. 4(i), are underlined. In these figures, some of the numbers of charges were omitted if they are always zero or less meaningful. Apparently, even the vacancy located in the ninth layer affected these charges around the dimers. This effect intensifies if the vacancy moves to the surface. Artificial interaction between the vacancy and the hydrogen-termination at the backside of models also affects the charges at the dimer surface. However, this effect can be canceled by comparisons among Figs. 4(a)–4(i).

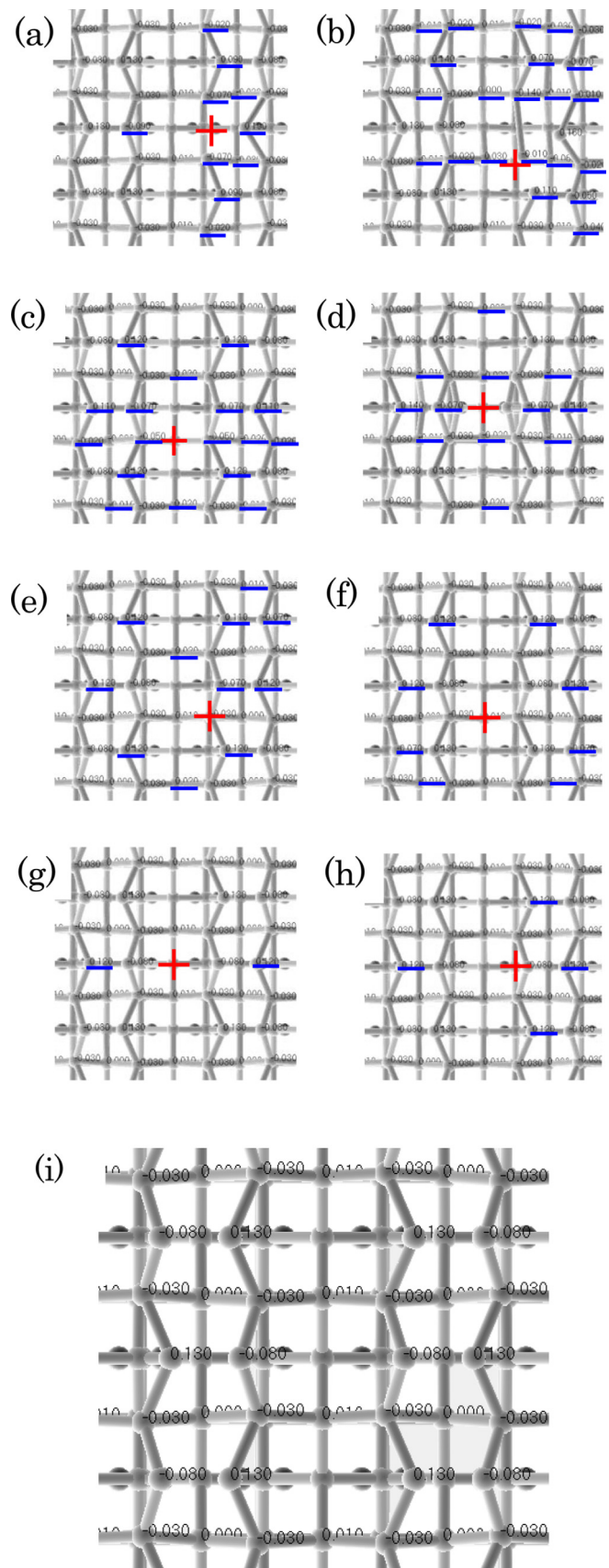


FIG. 4. (Color online) The changes of charges in atoms from first to fourth layers against vacancy introducing position in: (a) first, (b) second, (c) third, (d) fourth, (e) fifth, (f) sixth, (g) eighth, and (h) ninth layers, and (i) nowhere. These figures are top views, seen from the surface, and the projections of the original vacancy positions are marked with crossing lines. The different numbers of charges from (i) are underlined.



TABLE I. Distances in each component between atoms next to introduced vacancy sites: Atoms #1 ( $x_1, y_1, z_1$ ), and #2( $x_2, y_2, z_2$ ) are above the vacancy site. Atoms #3 ( $x_3, y_3, z_3$ ), and #4( $x_4, y_4, z_4$ ) are below the vacancy site. Each underline indicates that the value is dominant among the three components (unit: angstrom).

V position	x1-x2	y1-y2	z1-z2	x3-x4	y3-y4	z3-z4	z1-z3	z2-z4
2	0.732	2.129	0.595	3.882	0.115	0.441	1.835	1.681
3	4.106	0.000	0.000	0.000	3.909	0.007	2.646	2.638
4	0.000	3.592	0.000	2.958	0.000	0.000	3.145	3.145
5	—	—	—	—	—	—	—	—
6	0.042	3.871	0.047	3.772	0.002	0.002	2.705	2.660
7	3.755	0.000	0.000	0.000	3.786	0.005	2.606	2.611
8	0.000	3.904	0.000	3.846	0.000	0.000	2.583	2.583
9	3.826	0.000	0.091	0.000	3.823	0.000	2.624	2.714

Tables I and II enumerate the distances of each component and the charges of the atoms next to the introduced vacancy site, respectively. Similar to the vacancies in a bulk, the distances are smaller than those without distortions. If the introduced vacancy approaches the fourth layer from the bottom, the distances decrease. In addition, a Jahn-Teller distortion, i.e., the difference in distances between the above and the below atoms, also increases. This distortion decreases the total energy, as seen in Fig. 2. The distortion also caused the asymmetric charge distributions around the vacancy as shown in Table II, as the results of the interaction with charges of the dimer surface.

The increase in the total energy as a vacancy approaches the bottom is due to the convenience constraint of the Si atoms and this increase is nonsense. Models in which a vacancy is introduced in the first/second layer can reconstruct the atoms of their surface dimers and become more stable. As a result, the third layer, in which forming a vacancy requires the highest energy, becomes a singularity layer in a Si (100) surface with dimer structures. This means there is a potential diffusion barrier for the vacancies generated at the surface to the internal direction. In point defect simulations for Si wafers, boundary conditions of the point defect concentrations at the surface are often set at thermal equilibrium values inside the bulk without having any reasonable grounds.<sup>22</sup> The results obtained here, however, suggest the boundary condition at the surface should not be set at thermal equilibrium values in the Si bulk but considered as an infinite source (or the density of vacancies is equal to the

TABLE II. Electric charges in atoms next to introduced vacancy sites: Atoms #1 are above the vacancy site. Atoms #3, and #4 are below the vacancy site.

V position	#1	#2	#3	#4
2	0.11	-0.01	0.03	-0.06
3	-0.05	-0.05	0.02	0.04
4	-0.02	-0.02	0.00	0.00
5	—	—	—	—
6	0.00	0.10	0.20	0.20
7	0.00	0.00	-0.30	-0.30
8	0.10	0.10	-0.20	-0.20
9	-0.10	-0.10	-0.30	-0.30

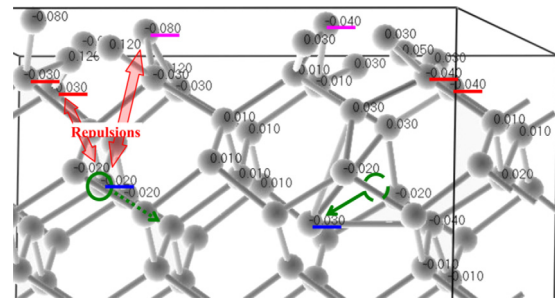


FIG. 5. (Color online) Obtained detailed structure and charges of model, in which vacancy is introduced in fifth layer from surface as initial structure. This includes a similar structure before the vacancy is introduced on the left side, which is the mirror image of the right side. We can see a clear interaction (“repulsions”) between the vacancy-originated charges and the surface dimer-originated one.

density of the atoms) with a potential barrier, like Si (100) asymmetric dimer structures that have a third layer.

As mentioned before, the model, in which a vacancy is introduced into the fifth layer from the surface as an initial structure, came to have a vacancy at the fourth layer as an optimized structure due to the movement of a Si atom from the fourth to the fifth layer. The right side of Fig. 5 shows the obtained detailed structure and charges of this model. This figure also includes a similar structure before a vacancy is introduced on the left side, which is a mirror image of the right side. We can see a clear interaction (“repulsions”) between the vacancy-originated and the surface dimer-originated charges. In particular, the top atom with the charge (-0.080) in Fig. 5 is the key for the atom in the fourth layer to completely move to the fifth layer. Consequently, the nature of the interaction between a surface dimer and a vacancy is intermediated by their accompanying charges.

## II. CONCLUSION

We investigated the interactions between the dimer structures of a reconstructed Si (100) surface and a vacancy to understand the behavior of the point defects near the surface using first principles calculations. We fabricated a model of a  $c(4 \times 2)$  structure, one of the most stable structures of a Si (100) surface. The calculation results showed that a vacancy located even in the ninth layer from the surface affects the charges around the dimers. This effect intensifies if the vacancy moves to the surface. Similar to vacancies in a bulk, a Jahn-Teller distortion occurred between the atoms around the vacancy. When the introduced vacancy approaches the fourth layer from the bottom, this distortion also increases, and thus decreases the total energy. The third layer, in which forming a vacancy requires the highest energy, becomes a singularity layer in a Si (100) surface with dimer structures. This means there is a potential diffusion barrier for the vacancies generated at the surface to the internal direction.

The model, in which a vacancy is introduced in the fifth layer from the surface, came to have a vacancy at the fourth layer as an optimized structure due to a Si atom moving from the fourth to the fifth layer. We can see a clear interaction between the vacancy-originated and the surface dimer-originated charges in this movement. As a result, the nature

of the interaction between a surface dimer and a vacancy is intermediated by their accompanying charges.

- <sup>1</sup>T. R. Anthony, *J. Appl. Phys.* **58**, 1240 (1985).  
<sup>2</sup>T. Yonehara, K. Sakuguti, and N. Sato, *Appl. Phys. Lett.* **64**, 2108 (1994).  
<sup>3</sup>M. Bruel, B. Aspar, and A. J. Auberton-Herve, *Jpn. J. Appl. Phys.* **36**, 1636 (1997).  
<sup>4</sup>K. Izumi, M. Doken, and H. Ariyoshi, *Electron. Lett.* **14**, 593 (1978).  
<sup>5</sup>S. Nakashima and K. Izumi, *J. Mater. Res.* **7**, 788 (1992).  
<sup>6</sup>O. W. Holland, D. Fathy, and D. K. Sadana, *Appl. Phys. Lett.* **69**, 674 (1996).  
<sup>7</sup>B. Doris, Y. Zhang, D. Fried, J. Beintner, O. Documaci, W. Natze, H. Zhu, D. Boyd, J. Holt, J. Petrus, J.T. Yates, T. Dyer, P. Saunders, M. Steen, E. Nowak and M. Jeong, *Dig. Tech. Pap.- Symp. VLSI Technol.* 86 (2004).  
<sup>8</sup>T. Shinno, *Semiconductor Silicon 2002*, edited by H. R. Huff, L. Fabry and S. Kishino (The Electrochemical Society, Pennington, N. J., 2002), PV 2002-2, p. 212.  
<sup>9</sup>E. Kamiyama and K. Sueoka, *J. Electrochem. Soc. H* **323**, 157 (2010).  
<sup>10</sup>R. M. Tromp, R. J. Hamers, and J. E. Demuth, *Phys. Rev. Lett.* **55**, 1303 (1985).  
<sup>11</sup>R. J. Hamers, R. M. Tromp, and J. E. Demuth, *Phys. Rev. B* **34**, 5343 (1986).  
<sup>12</sup>R. A. Wolkow, *Phys. Rev. Lett.* **68**, 2636 (1992).  
<sup>13</sup>P. Hohenberg and W. Kohn, *Phys. Rev.* **136**, B864 (1964).  
<sup>14</sup>W. Kohn and L. Sham, *Phys. Rev.* **140**, A1133 (1965).  
<sup>15</sup>D. Vanderbilt, *Phys. Rev. B* **41**, 7892 (1990).  
<sup>16</sup>B. Hammer, L. B. Hansen, and J. K. Norskov, *Phys. Rev. B* **59**, 7413 (1999).  
<sup>17</sup>The CASTEP code is available from Accelrys Software Inc.  
<sup>18</sup>G. Kresse and J. Furthmuller, *Phys. Rev. B* **54**, 11169 (1996).  
<sup>19</sup>T. Fischer and J. Almlof, *J. Phys. Chem.* **96**, 9768 (1992).  
<sup>20</sup>H. Monkhorst and J. Pack, *Phys. Rev. B* **13**, 5188 (1976).  
<sup>21</sup>R. S. J. Mulliken, *Chem. Phys.* **23**, 1833 (1955).  
<sup>22</sup>K. Nakamura, T. Saishoji, T. Kubota, T. Iida, Y. Shimanuki, T. Kotooka, and J. Tomioka, *J. Cryst. Growth* **180**, 61 (1997).